Electronic Supplementary Material (ESI) for Journal of Materials Chemistry A.

Raspberry-Like Mesoporous Co-Doped TiO_2 Nanospheres for High-Performance Formaldehyde Gas Sensor

Qian Rong,[a] Yuan Li,*[b] Shiqiang Hao,[c] Songting Cai,[c] Chris Wolverton,[c] Vinayak P. Dravid,[c] Tianyou Zhai, [b] Qingju Liu*[a]

[a] School of Physics and Astronomy, School of Materials and Energy, Yunnan Key Laboratory for Micro/Nano Materials & Technology, National Center for International Research on Photoelectric and Energy Materials, Yunnan University, Kunming 650091, China

[b] State Key Laboratory of Material Processing and Die & Mould Technology, School of Materials Science and Engineering, Huazhong University of Science and Technology, Wuhan, Hubei 430074, China

[c] Department of Materials Science and Engineering, Northwestern University, Evanston, Illinois 60208, USA

S1. Experimental Section

S1.1. Materials characterization

Polyvinylpyrrolidone (PVP_{36000}, Mw = 36000), cobalt nitrate ($Co(NO_3)_2 \cdot 6H_2O$), tetrabutyl titanate (TBOT), and pluronic F127 were purchased from Aladdin; the styrene, phenol, formaldehyde solution, acetic acid and hydrochloric acid were purchased from Sigma-Aldrich and used without any further purification. The crystal structures of the r-Co-TiO_2 were analyzed with the X-ray diffractometer with Cu-Kα radiation (λ=1.54056 Å). Sample morphologies were recorded with field emission scanning electron microscopy (FESEM 450, Thermo Fisher Scientific Co. Ltd.) and transmission electron microscope (TEM, JEOL 300F and 200 kV). The element composition of the porous Co doped TiO_2 microspheres were determined by quantitative X-ray spectroscopy (EDS) capabilities attached to the TEM equipped. Brunauer-Emmett-Teller surface area (BET_{area}) and pore size volume and distributions were performed using N_2 adsorption/desorption isotherms (($N_{2ads/des}$ curve, Quadrasorb-evo equipment) at 77 K. X-ray photoelectron spectra (XPS) were carried out K-Alpha+ spectrometer (1486.6 eV) using Al Kα excitation, and calibrated using the C 1s peak at 284.8 eV as a charge reference.

S1.2. Synthesis of honeycomb carbon scaffolds

First, 16 g of styrene, 0.15 g of PVP_{36000} was dissolved in 130 mL of ethanol and water mixed solution, and then 3.20 g of ammonium peroxydisulfate was slowly added into above solution. The mixed solution was transferred to 200 mL round bottom flasks and stirred at 80°C for 5 h in in N_2 atmosphere by using a mechanical stirrer. The obtained polystyrene colloids were washed with ethanol and dispersed in 200 mL of ethanol. Afterward, 16 g of phenol was melted at 50°C, then 4 g of 30 wt% NaOH solution was added into a phenol solution, after 30 min under stirring, 36.8 mL of formaldehyde solution was quickly added, and stand at 80°C for 2 h, the pH of this solution was adjusted to 6 with 5 mL HCl. The solution was dried at 50°C

for 10 h to obtained phenolic resin sol gel, and the sol gel was dispersed by ethanol. Finally, 10 mL of phenolic resin solution was dropwise added to 20 mL Polystyrene sphere under magnetic stirring for 12 h at room temperature, the mixed solution was dried at 75°C followed by further annealed at 500°C for 6 h in N_2/O_2 atmosphere in order to obtain the three-dimensional honeycomb carbon scaffolds (3D HCS).

S1.3. Synthesis of raspberry-like mesoporous Co-doped TiO_2 (r-Co-TiO_2) nanospheres

The detailed synthesis process was illustrated in Figure 1. Briefly, 3 g of Plouronic F127 was firstly mixed with 20 mL of HCl and 40 mL of ethanol, then stirred at room temperature for 5 h to obtained clear and transparent solution. Sequentially, 6.8 g TBOT and 0.15 g $Co(NO_3)_2 \cdot 6H_2O$ mixed into the above solution under stirring for 1 h to form transparent blue solution, and dried under 80°C for 24 h to obtain blue sol gel. A control sample Co-doped TiO_2 sphere (namely c-Co-TiO_2) was achieved by calcining blue sol gel at 450°C for 2 h with a heating rate of 5 °C min^{-1}. Finally, the 3-dimentional honeycombed with carbon scaffolds soaked into blue mixture solution and underwent freeze-drying for about 48 h, the impregnated honeycomb carbon scaffolds were heated at 300°C (2°C min^{-1}) for 4 h under N_2 atmosphere. The temperature is then further increased to 400°C for 5 h to obtained the Co-doped TiO_2 nanospheres (Co-TiO_2), which were further subjected to another deep annealing for 6 h to obtain the raspberry-like Co-doped TiO_2 nanospheres (r-Co-TiO_2).

S1.4. Gas sensor fabrication and measurements

5 mg of c-Co-TiO_2, Co-TiO_2 and r-Co-TiO_2 nanosphere powders were dispersed in the 5 mL of printing oil. Then, the paste of each sensing material was applied on a substrate (30 mm × 6 mm × 0.625 mm) by mechanically automated screen-printing technology. Before measurements, the sensor was stabilized under 325°C for 2 h in air. The formaldehyde gas performance of the sensor was tested in a sealed cavity. The formaldehyde gas performance of the sensor was tested by HCRK-SD101 gas sensing analyzer (Wuhan HCRK Technology Co.

Ltd.) in the temperature range of 50-200°C with the relative humidity of 20%-30%. The formaldehyde liquid was injected on the evaporation table in the chamber of the gas sensing analyzer. Assumed under standard atmospheric pressure, the concentration of the formaldehyde was calculated according to the volume of the formaldehyde liquid and the chamber at room temperature. Therefore, different concentrations of formaldehyde can be obtained by controlling the volume of the liquid. The concentration of other organic volatile gases was obtained similarly. The sensitivity of the gas sensor can be defined as the ratio of the resistance value (Ra) in the fresh air to the resistance value (Rg) in the tested gas. Response and recovery times refer to the time required to achieve 90% of the maximum sensing value during adsorption and desorption, respectively. To confirm the selectivity of the sensors, the response of sensors to 10 ppm of methanol, ethanol, acetone, benzene and gasoline were also investigated, respectively. The limit of detection (LD) is a vital parameter to characterize a sensor which defines about the minimum amount that a sensor can sense. The limit of detection (LD) is calculated by using the formula, $LD = 3\frac{Rmsd}{S}$, where Rmsd is the root-mean-square deviation and S is the slope of the calibration curve.

S1.5. Density Functional Theory details

We use plane-wave density functional theory (DFT) for the energy calculations of all relaxed structures. Our DFT calculations are carried out with the PBE-GGA functional *via* the Vienna ab initio simulation package (VASP), with the Projector Augmented-Wave pseudopotentials defined within VASP. For adsorbant on the surface structure optimizations, we create slabs with at least 15 Å vacuum spaces. For total energy calculations, the cutoff energy for all calculations was 500 eV. Energy minima were located *via* geometry optimization in which atoms were relaxed until the forces on all atoms were less than 0.03 eV/Å. For each minimum, the molecular adsorption energy was defined by $E_{ads} = E_{tot} - E_{slab} - E_g$, where E_{tot} and E_{slab} are the total energies of slabs with and without the adsorbed species present, and E_g is

the total energy of molecular species in the gas phase. With this convention, negative adsorption energies define states that are energetically favorable relative to the gas phase molecule and the clean surface. For the dissociation and diffusion processes, a standard chain-of-states method such as the Nudged Elastic Band (NEB) method was applied to locate transition states and energy barriers.

S2. Supplementary Tables

Table S1 Comparison of key sensing parameters of various formaldehyde gas sensors in this study as well as the recently-reported literature.

Materials	Formaldehyde (ppm)	Working temperature (°C)	t_{res}/t_{rec} (s)	Response (R_g/R_a)	References
r-Co-TiO_2	10	86	26.4/18.2	84.8	This work
Mesoporous α-Fe_2O_3	1	300	63/395	5.7	[1]
Co_3O_4/ZnO	10	120	42/23	6.17	[2]
$(Ga_{0.2}In_{0.8})_2O_3$	100	200	1/1	50	[3]
$Al_{0.15}In_{1.85}O_3$	100	150	23/103	60.3	[4]
Pd-WO_3/g-CN	25	120	6.8/4.5	24.2	[5]
$La_{0.75}Sr_{0.25}Cr_{0.5}Mn_{0.5}O_{3-\delta}$-$SnO_2$	5	400	32/231.2	26.5	[6]
In_2O_3/1% Co nanorods	10	130	60/120	23.2	[7]
SnO_2/In_2O_3	50	300	60/97	118	[8]
CuO-TiO_2	50	200	1.4/	15.5	[9]
Co_3O_4	3	150	279/564	8.2	[10]
Ag/$LaFeO_3$	1	125	90/80	18.6	[11]

Table S2 The adsorption energy of TiO_2 and Co-TiO_2 for different test gases.

Test gas	Co-TiO_2	TiO_2
Formaldehyde	-0.058	0.36
Methanol	0.026	0.29
Ethanol	0.52	0.76
Acetone	-0.024	0.27
Benzene	0.15	0.41

References

1 H. J. Park, S. Y. Hong, D. H. Chun, S. W. Kang, J. C. Park, D. S. Lee, *Sens. Actuators B. Chem.* 2019, **287,** 437.

2 J. Sun, L. Sun, S. Bai, H. Fu, J. Guo, Y. Feng, R. Luo, D. Li, A. Chen, *Sens. Actuators B. Chem.* 2019, **285,** 291.

3 T. Wang, B. Jiang, Q. Yu, X. Kou, P. Sun, F. Liu, H. Lu, X. Yan, G. Lu, *ACS Appl. Mater. Interfaces* 2019, **11,** 9600-9611.

4 H. Chen, Y. Zhao, L. Shi, G. D. Li, L. Sun, X. Zou, *ACS Appl. Mater. Interfaces* 2018, **10,** 29795-29804.

5 R. Malik, V. K. Tomer, T. Dankwort, Y. K. Mishra, L. Kienle, *J. Mater. Chem. A.* 2018, **6,** 10718-10730.

6 J. Y. Kang, J. S. Jang, W. T. Koo, J. Seo, Y. Choi, M. H. Kim, D. H. Kim, H. J. Cho, W. Jung, I. D. Kim, *J. Mater. Chem. A.* 2018, **6,** 10543-10551.

7 Z. Wang, C. Hou, Q. De, F. Gu, D. Han, *ACS sensors* 2018, **3,** 468.

8 J. Liu, X. Li, X. Chen, H. Niu, X. Han, T. Zhang, H. Lin, F. Qu, *New J. Chem.* 2016, **40,** 1756.

9 J. Deng, L. Wang, Z. Lou, T. Zhang, *J. Mater. Chem. A* 2014, 2, 9030.

10 J. Y. Kim, N. J. Choi, H. J. Park, J. Kim, D. S. Lee, H. Song, *J. Phys. Chem. C* 2014, 118, 25994.

11 Y. Zhang, Q. Liu, J. Zhang, Q. Zhu, Z. Zhu, *J. Mater. Chem. C* 2014, 2, 10067.

S3. Supplementary Figures

Fig. S1 Fundamental chemical reaction mechanism for the synthesis of c-Co-TiO_2.

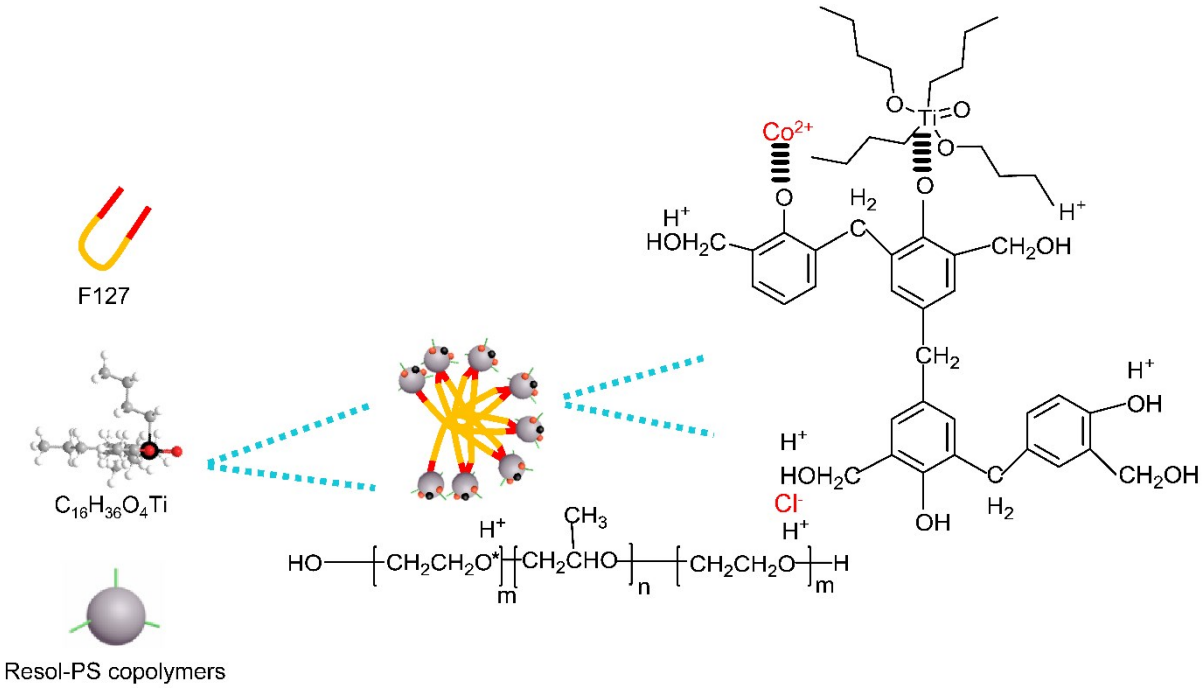

Fig. S2 SEM images of the honeycomb carbon template under different magnification.

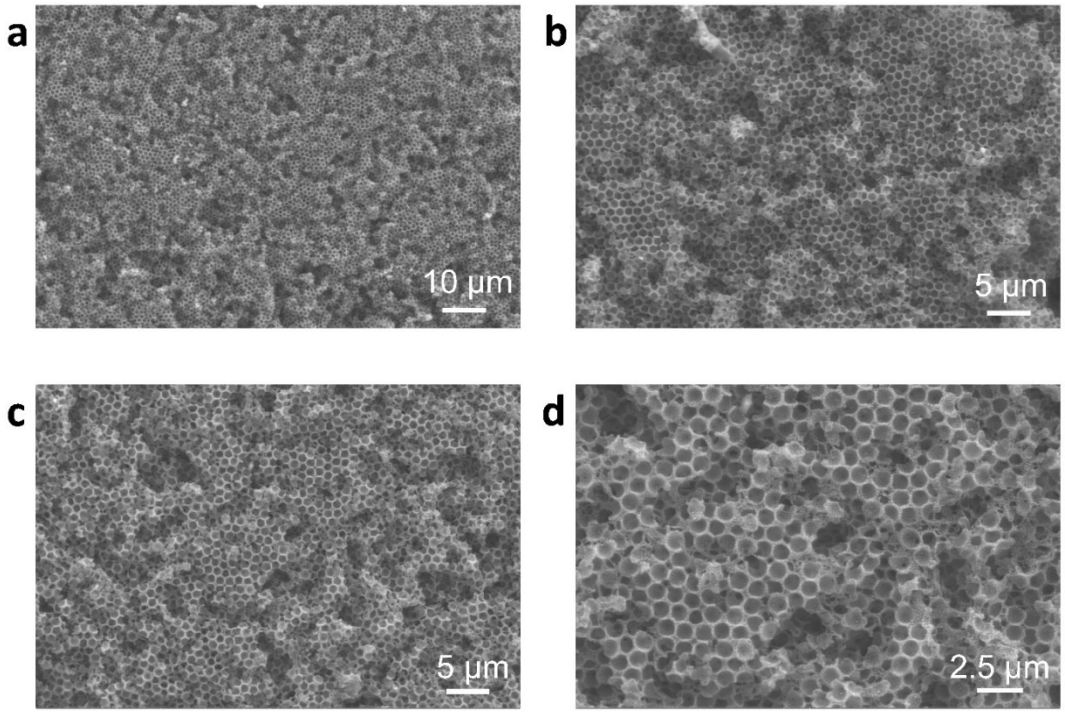

Fig. S3 SEM images of the Co-TiO_2 (after step d in Fig. 1) under different magnifications.

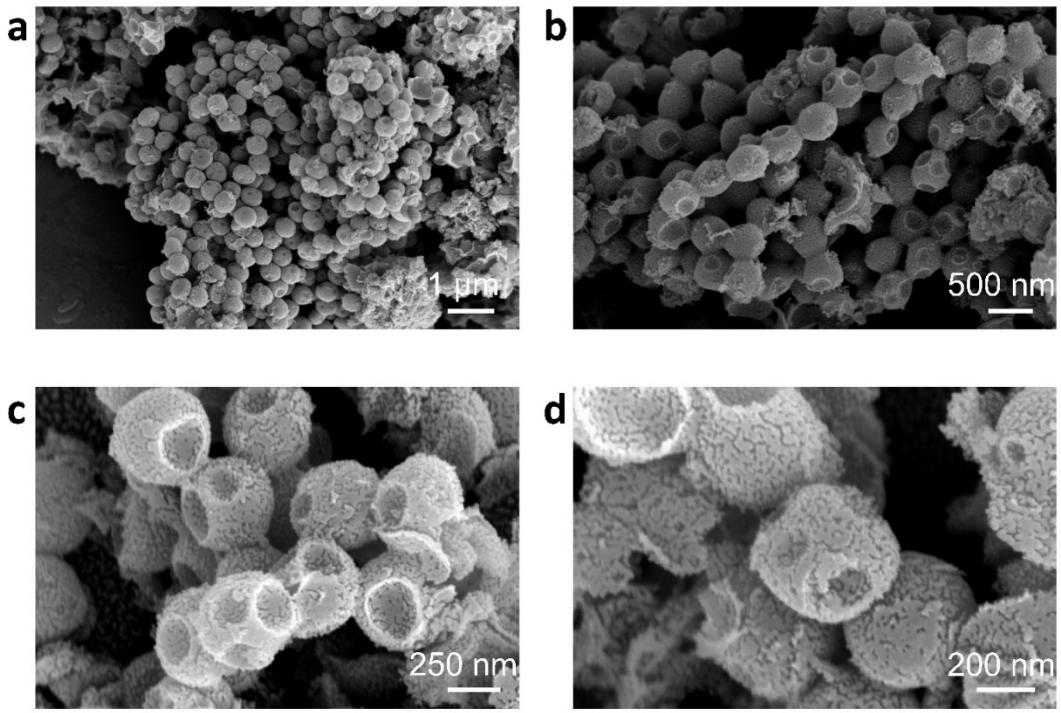

Fig. S4 SEM images of the r-Co-TiO_2 (after the deep annealing step e in Fig. 1) under different magnifications.

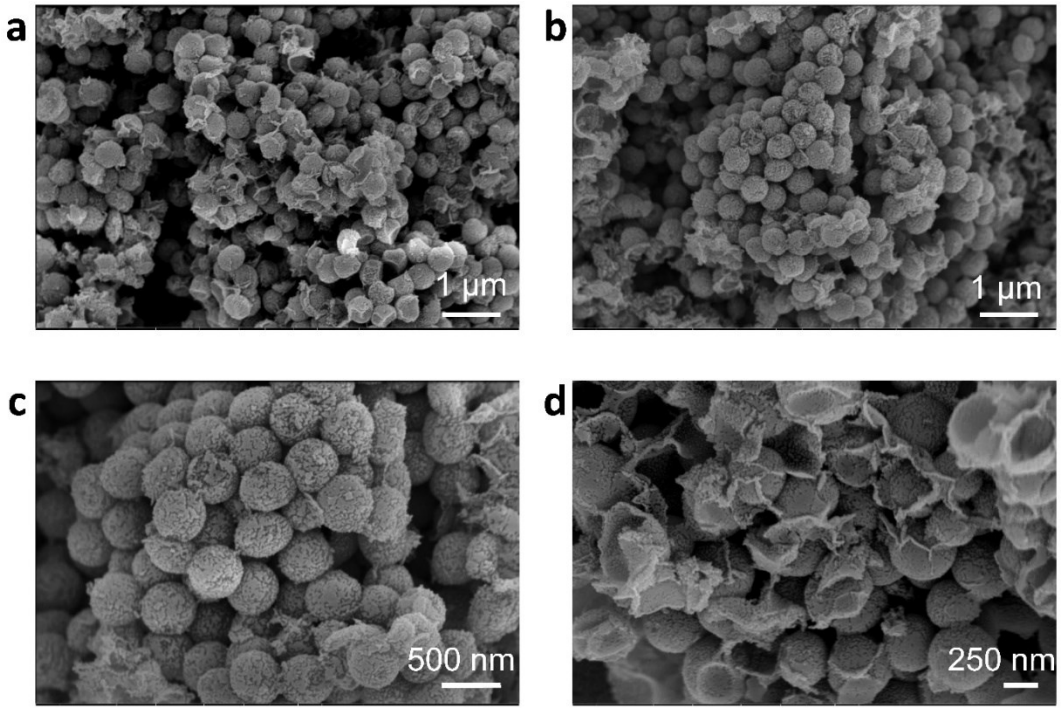

Fig. S5 SEM images of the c-Co-TiO_2 (without use of the honeycomb carbon template) under different magnifications.

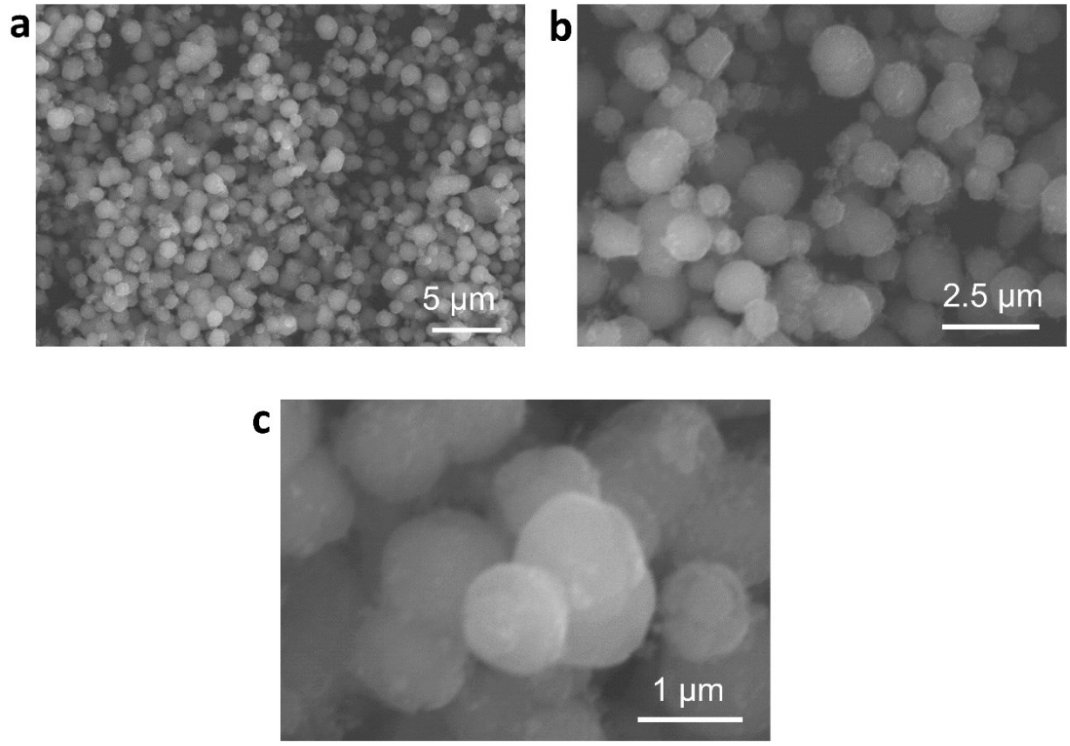

Fig. S6 (a) XPS full spectrum, (b-d) XPS spectra of Ti 2p (b), Co 2p (c) and O 1s (d) for the c-Co-TiO_2.

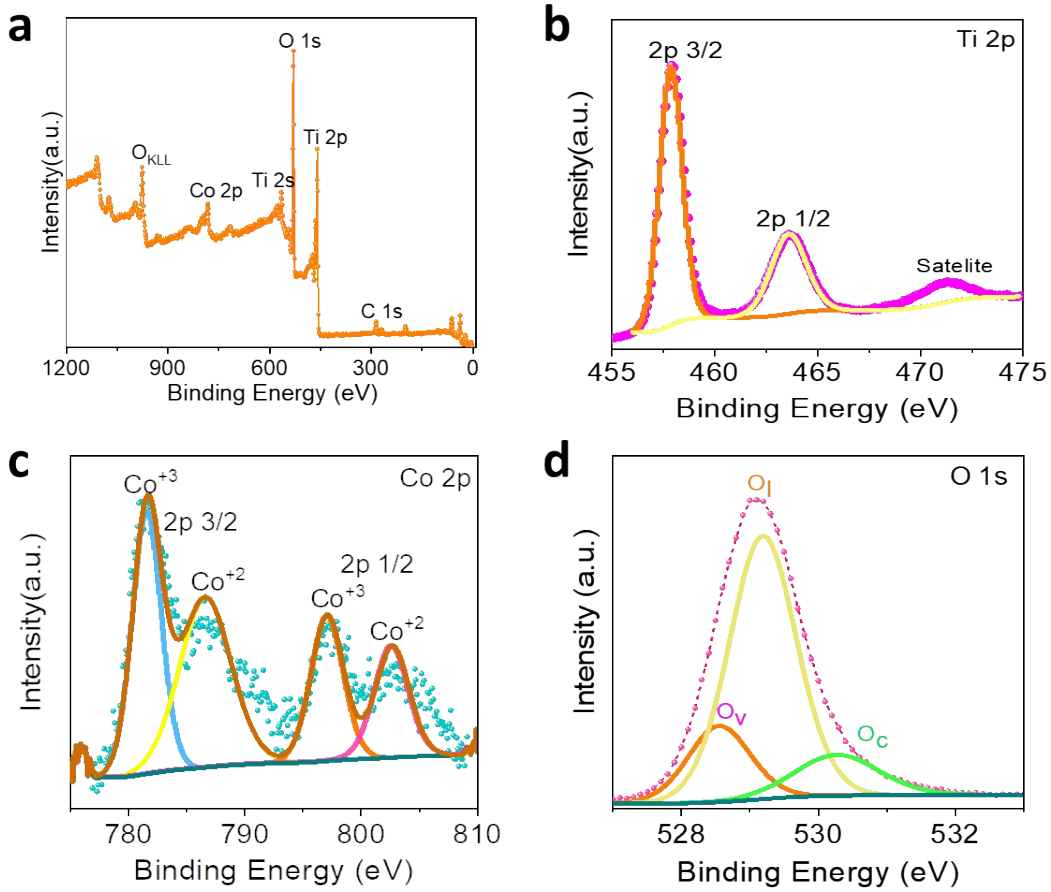

Fig. S7 The response of various gas sensors at different temperature. (a) r-Co-TiO_2, (b) Co-TiO_2, (c) c-Co-TiO_2, (d) c-TiO_2 for 10 ppm of various gas molecules.

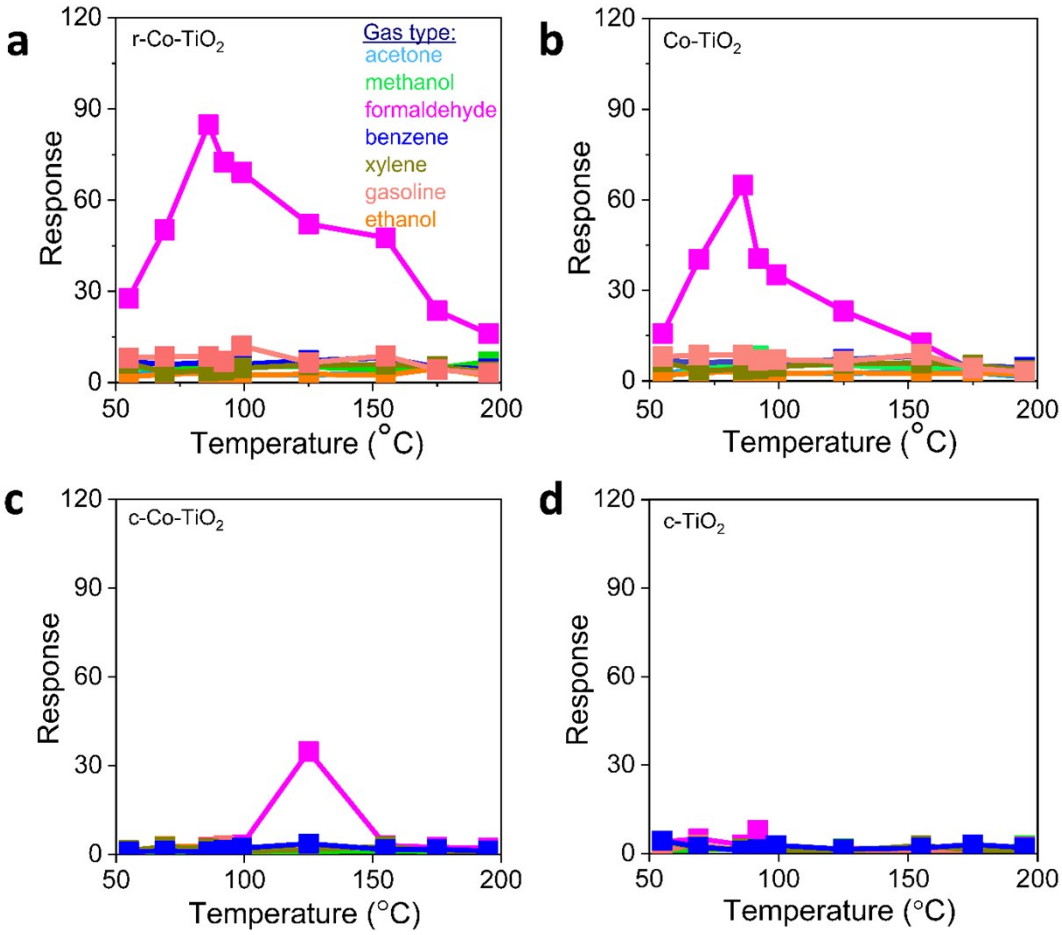

Fig. S8 Response-time plots of various gas sensors under increasing formaldehyde concentration. (a) r-Co-TiO_2, (b) Co-TiO_2, (c) c-Co-TiO_2, (d) c-TiO_2.

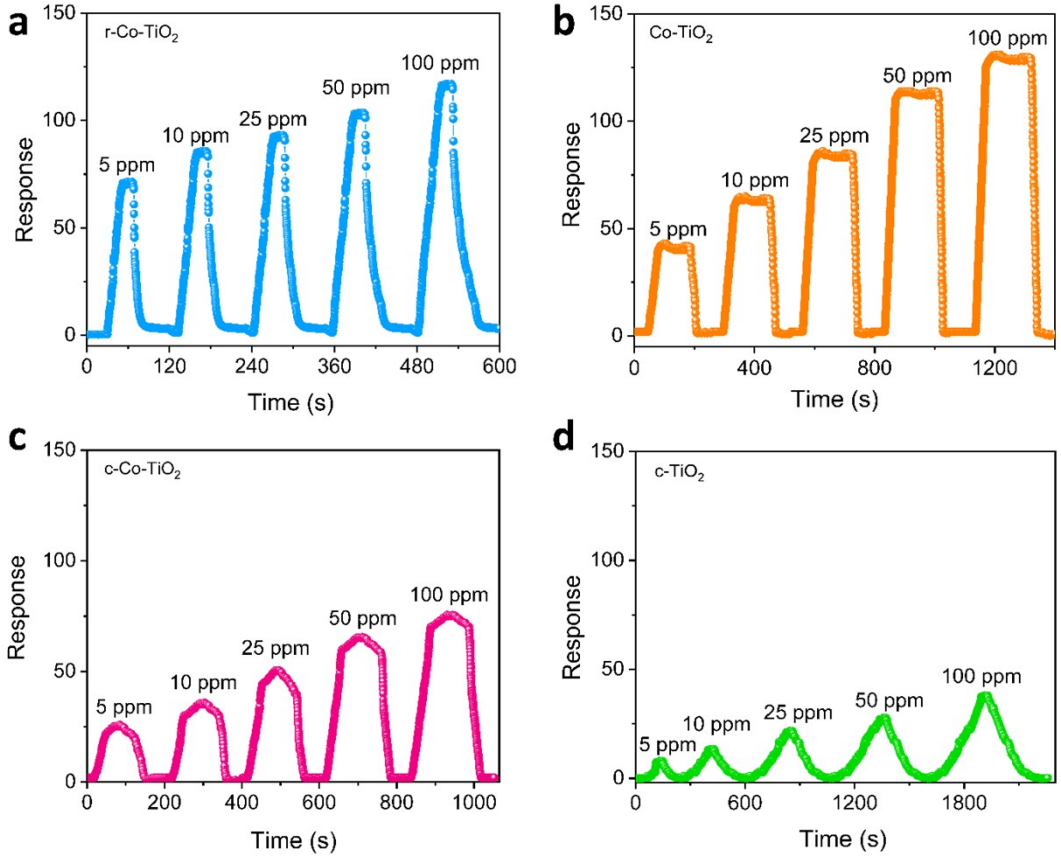

Fig. S9 Response-time curves of various gas sensors for long-time operation. (a) r-Co-TiO_2, (b) Co-TiO_2, (c) c-Co-TiO_2, (d) c-TiO_2.

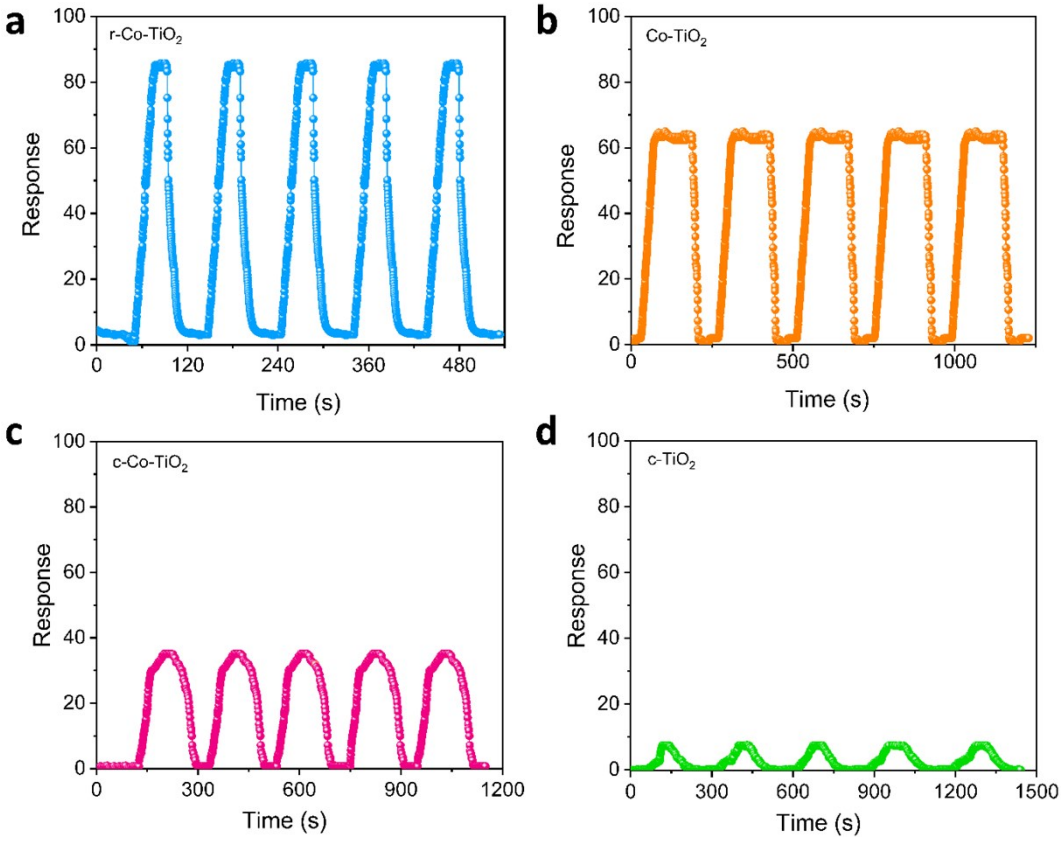

Fig. S10 Response-time plots indicating the response rate (rise time and decay time) of various gas sensors. (a) r-Co-TiO_2, (b) Co-TiO_2, (c) c-Co-TiO_2, (d) c-TiO_2.

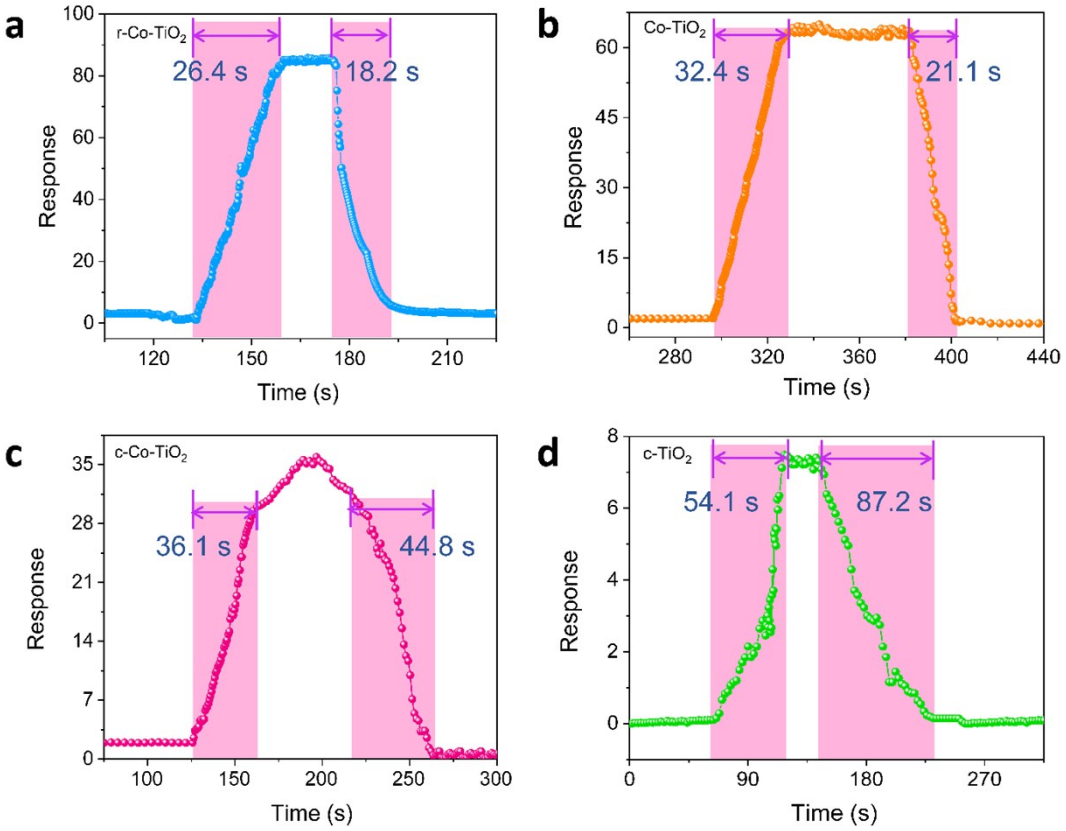

Fig. S11 (a) Responses of r-Co-TiO_2 sensors to 10 ppm formaldehyde in the relative humidity range from 20 to 80% at 86 °C, (b) long-term stability of the sensor to 10 ppm formaldehyde gas.

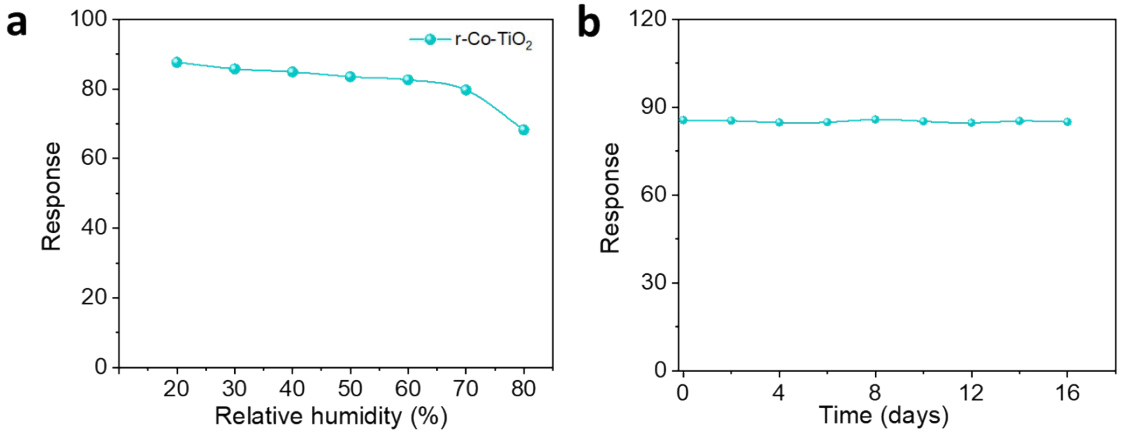

Fig. S12 DFT calculation of the electronic structure. (a-c) The calculated electronic structure for the pristine TiO_2, oxygen-absorbed TiO_2 and formaldehyde-absorbed TiO_2. (d-f) The calculated electronic structure for the pristine Co-TiO_2, oxygen-absorbed Co-TiO_2 and formaldehyde-absorbed Co-TiO_2.

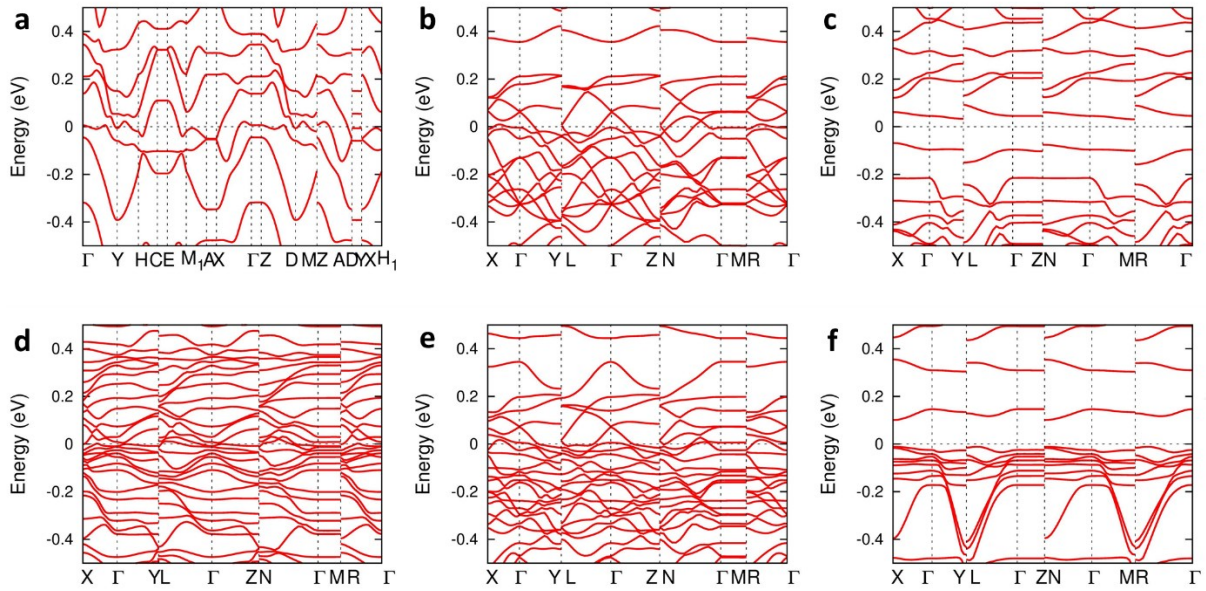

Fig. S13 Schematic illustrating the gas-sensing mechanism. (a-c) The variation of surface metallic layer on TiO_2. (d-f) The variation of surface metallic layer on Co-TiO_2.